Marine Pollution Bulletin 220 (2025) 118346

Contents lists available at ScienceDirect

Marine Pollution Bulletin

journal homepage: www.elsevier.com/locate/marpolbul

Effects of chemical leachates from offshore wind farm infrastructure on heart rate and valve gape of blue mussels

Katharina Alter [a,b,*], Moses Ndugwa [c], Paula de la Barra [a,d], Lieven Bervoets [c], Gudrun De Boeck [c], Andy M. Booth [e], Lisbet Sørensen [e,f]

[a] Department of Coastal Systems, Royal Netherlands Institute for Sea Research (NIOZ), PO Box 59, 1790 AB Den Burg, (Texel), the Netherlands
[b] Department of Marine Biology, Institute of Biological Sciences, University of Rostock, Rostock, Germany
[c] ECOSPHERE, Department of Biology, University of Antwerp, Antwerp, Belgium
[d] UK Centre for Ecology and Hydrology, Bangor, United Kingdom
[e] Department of Climate and Environment, SINTEF Ocean, Trondheim, Norway
[f] Department of Chemistry, Norwegian University of Science and Technology (NTNU), Trondheim, Norway

ARTICLE INFO

Keywords:
Chemical mixtures
Stress indices
Toxicity
Ecotoxicology
CTmax
Pollution
PAHs

ABSTRACT

Offshore wind farms (OWFs) play a key role in combating climate change, but the coatings used to protect submerged infrastructure can leach potentially harmful chemicals into the marine environment. These leachates may affect marine species colonizing OWF structures or being cultured near OWFs, such as blue mussels. To assess the impacts, we monitored valve gape behaviour and heart rate in *Mytilus edulis* exposed to coating leachates under controlled conditions, followed by a thermal ramping to assess potential constraints in their stress performance. Using non-targeted screening with two-dimensional gas chromatography and high-resolution mass spectrometry, we identified nine chemicals in the leachates plausibly assigned to the coatings, including alcohols, ketones, lactones, bromobenzenes, dibromophenols, and polycyclic aromatic hydrocarbons. At constant temperatures, exposed mussels showed both up to 12 % reduced and up to 18 % increased daily cardiac arrest compared to control mussels. However, during cardiac activity heart rate and valve gape were similar among treatments. Leachate exposure did not lead to reductions in fitness endpoints during the thermal ramping, i.e. the temperature at which heart rate was maximal (21.3 ± 0.4 °C) and valves started to close (19.2 ± 0.6 °C). Non-targeted screening does not allow for comparisons of chemical concentrations from field samples, yet the painted surface to volume of seawater ratio used here potentially led to much higher leachate concentrations than any environmentally relevant conditions. Future research on leachates from other OWF sources, such as sacrificial anodes, is needed to gain a comprehensive understanding of ecological risks and support sustainable OWF development.

1. Introduction

To combat climate change, countries worldwide increase their carbon-neutral energy production by investing in renewable energy sources, including wind energy. With record-setting years occurring in 2020 and 2021, the global capacity for wind farms has been steadily increasing, not only for land but also offshore. However, the current growth rate for renewable energy needs to increase fourfold if society is to meet the targets of the Paris Agreement and the European Union Green Deal, which aims for net-zero emissions by 2050 (Global Wind Energy Council, 2022).

Foundations and transition pieces of the turbine pillars in an offshore wind farm (OWF) are submerged and must withstand the impacts of the corrosive marine environment for a period of time that exceeds their service life (Eom et al., 2020; Price and Figueira, 2017). A combination of corrosion protective coatings and sacrificial anodes is therefore used to minimize the risk of corrosion and material fatigue. The coatings prevent the direct contact of the metal structure with the environment while the sacrificial anodes reduce the metal corrosion rate when the coating is damaged. The coatings typically consist of several layers of

* Corresponding author at: Department of Coastal Systems, Royal Netherlands Institute for Sea Research (NIOZ), PO Box 59, 1790 AB Den Burg, (Texel), the Netherlands.
E-mail addresses: Katharina.alter@uni-rostock.de (K. Alter), Moses.Ndugwa@uantwerpen.be (M. Ndugwa), paudel@ceh.ac.uk (P. de la Barra), lieven.bervoets@uantwerpen.be (L. Bervoets), gudrun.deboeck@uantwerpen.be (G. De Boeck), andy.booth@sintef.no (A.M. Booth), lisbet.sorensen@ntnu.no (L. Sørensen).

https://doi.org/10.1016/j.marpolbul.2025.118346
Received 28 April 2025; Received in revised form 20 June 2025; Accepted 22 June 2025
Available online 1 July 2025

organic coat or a combination of metal and organic coat (Eom et al., 2020, Price and Figueira, 2017).

Offshore wind farms are not typically considered as sources of pollutant emissions, especially as the use of some common coating ingredients (e.g. zinc chromate, red lead, calcium plumbates) with known risks to human health and the environment are already restricted (Abramic et al., 2022; Price and Figueira, 2017). Over time, however, chemicals used in OWF coatings can leach into the surrounding seawater whereby the process and rate is dependent on local environmental conditions (Yu et al., 2021; Eom et al., 2020). Once in the marine environment, these chemical leachates can be bioavailable to organisms. Although available reports about achieving good environmental status emphasize the need to determine baseline levels of OWF-related chemical contaminants in marine organisms (Abramic et al., 2022), no studies on OWF chemical contaminant concentrations in organisms have been published to date.

While the bioavailability and toxicity of chemicals can vary with changing environmental conditions (Nardi et al., 2017; Noyes and Lema, 2015), the inter-related effects of climate change and chemical pollution on marine organisms are rarely studied simultaneously. Also, the bioaccumulation of chemicals can depend on temperature, as the latter stimulates an increased metabolism that is often accompanied by increased feeding and thus an increased potential for chemical bioaccumulation (Maulvault et al., 2018; Alava et al., 2017). Arguably the most important influence, however, are the potential synergistic effects between the two drivers, i.e. warming and chemical pollution, that could result in increased susceptibility to chemicals or a decreased ability to withstand environmental changes, such as temperature peaks (Alava et al., 2017).

An ideal model species to study the effects of OWF-derived chemical leachates and warming are blue mussels because they are one of the dominating species colonizing the subtidal structures of OWFs. In addition, mussels are target species for aquaculture facilities located near to OWFs. They are highly sedentary, have a filter feeding life strategy, and they respond behaviourally and physiologically to environmental factors and chemical stressors (Durier et al., 2021; Degraer et al., 2020; Tran et al., 2020). Environmental and chemical stress can trigger shell movement and valve closure in mussels which are measurable indicators that are more sensitive than other traditional endpoints such as mortality and growth (Hartmann et al., 2016). Hence, valve closure can be used as a behavioural sign that reflects unfavourable conditions. By closing their valves, mussels prevent contact of their soft tissues with the surrounding environment, yet this defence mechanism also restricts food uptake and respiration. The reduction in oxygen tension can also lead to bradycardia (reduced heart rates) and mussels may eventually switch to an anaerobic metabolism (Kholodkevich et al., 2009; Braby and Somero, 2006). This can be an energy saving strategy, but when maintained for too long, can ultimately impact the mussels' vital rates (Riisgård and Larsen, 2015). Further, cardiac activity can also be used as a physiological indicator of general health and fitness (Bakhmet et al., 2021; Turja et al., 2014; Halldórsson et al., 2008). During exposure to a short-term thermal increase, for example, heart rate will increase until the temperature for maximal heart rate is reached (Alter et al., 2025). A sudden decrease after the performance maximum is indicative of cumulative cell damage caused by the foregone thermal stress and indicates the individuals' sublethal limit (Moyen et al., 2019).

Considering the large number and diversity of chemicals used in OWF corrosion protection coatings, it is difficult to assess the impact of all possible combinations of chemicals (Hengstmann et al., 2025). Therefore, we exposed the blue mussel, *Mytilus edulis*, to metal plates that were fully covered with the coating systems most commonly used for OWF installations to assess the impact of the combined effect of all chemical leachates. We monitored valve gape and heart rate of mussels continuously and determined the composition of the chemical leachate in seawater regularly. After a two-week exposure at a constant temperature of 13 °C, mussels were subjected to a gradual increase in temperature to assess potential interactions with OWF-derived leachates in the presence of an additional environmental driver. Because blue mussels are one of the dominating species colonizing the shallow subtidal structures of OWFs (Degraer et al., 2020), we hypothesized that exposure to chemical leachates from OWFs would not affect their valve gape and heart rate. However, even without measurable effects on the organismal level, exposure to chemical leachates may still affect mussels at the cellular level (Bordalo et al., 2023; Kasiotis et al., 2015), reducing the overall ability to withstand changes in environmental factors (Alava et al., 2017; Sokolova and Lannig, 2008). Thus, we hypothesized that when challenged with a thermal ramping, mussels that were previously exposed to chemical leachates would show lower fitness compared to control individuals.

2. Methods

2.1. Animal collection and husbandry

Adult *M. edulis* were supplied from a North Sea blue mussel farm (Colruyt Group) off the Belgian coast (Zeeboerderij Westdiep, N 51°09′924″ E 2°37′747″) in June 2023 and transported to the University of Antwerp. Mussels (approx. 500 individuals) were held in tanks (300 L, n = 2) filled with artificial seawater (hw-Marinemix professional, Wiegandt GmbH, Germany, in deionized water) at 13 °C, 33 salinity, with constant aeration, and a 12 h:12 h light: dark period. They were fed freeze dried microalgae (*Tetraselmis chuii*, TetraPrime C, Proviron, Belgium) at a concentration of 25,000 cells/mL every other day and water was renewed once a week.

2.2. Animal preparation and experimental design

Chemical exposure during stable temperature (hereinafter "coupon exposure"): In September 2023, mussels of similar size (n = 27, mean shell length ± SE: 58.0 ± 0.6 mm, range: 52.1–64.3 mm) were randomly selected from the holding tanks and used in experiments to test if exposure to chemical leachates from OWFs affects their heart rate and valve gape behaviour. Experiments took place in a temperature controlled room set to 13 °C and a 12 h:12 h light: dark period. In a glass aquarium (49 × 28 × 30 cm, L × W × H, n = 6), one stainless steel plate (10 × 20 × 0.3 cm) coated on all surfaces (Interthane 990 RAL 1003 (primer 1: Interzone 954 grey, primer 2: Interzone 954 white, top: Interthane), International) was placed in 20 L artificial seawater at 33 salinity. The two short sides of the plate were placed on a glass petri dish and contained a hole in which a glass tube was inserted for aeration and to ensure water circulation around the plate and throughout the aquarium. An aquarium served as direct (n = 3) or indirect (n = 3) exposure treatment by placing mussels (n = 3 per aquarium) either directly on the plate (direct) or around the plate without direct contact (indirect). Additional aquaria (n = 3 with n = 3 mussels each) without a plate served as control treatment. Before placing mussels in the aquaria, each individual was equipped with a wired heart rate sensor (Pulse V2, Electric Blue, Portugal) and a custom-built valve gape sensor (Ballesta-Artero et al., 2017) which were attached onto the shell above the heart and onto the posterior margin of both valves, respectively, using cyanoacrylate (Colle Seconde Lijm, Bison, the Netherlands). The heart rate sensor illuminated the heart with an infra-red light which was then reflected and detected by an infra-red sensor, recorded at a sampling rate of 10 Hz and stored in a log file (Pulse V2, Electric Blue, Portugal). The valve sensor consisted of paired electromagnetic coils that measured the strength of an electromagnetic field that existed between them. The strength of the field changed according to the distance between the two coils. The field was recorded at a sampling rate of 1 Hz and stored in a log file. Recording of heart rate and valve gape started immediately after deployment. During the following exposure period, mussels were fed (conditions as above) on experimental day 2, 5, 7, 9 and 12. Water was

exchanged (100 %) with reservoir water on day 5 and 10. In reservoir glass aquaria (100 × 40 × 50 cm, L × W × H, 140 L volume, n = 1 per treatment), painted plates were placed at the same ratio as in the exposure aquaria (1 plate/20 L sea water) to keep chemical compositions and -abundances similar between water exchanges. Duplicate water samples (250 mL) were taken from all three reservoir tanks on days 6, 7, 9, 12, 14 and 15. Samples were spiked with 15 % hydrochloric acid (HCl) and stored in glass bottles (Borosilicate 3.3 glass, VWR) with a Teflon-lined bottle cap (PBT with PTFE-coated gasket, Duran) and were kept in darkness at 13 °C. After termination of experiments, samples were frozen at −20 °C for later chemical analysis of leachates. Temperature, salinity, and oxygen level (WTW Multi 3620 IDS with TetraCon 925 and FDO 925 electrodes, Germany) in exposure aquaria were measured every other day. Apart from these maintenance procedures during which the presence of people in the room were noted, animals were left undisturbed.

Stress performance test: For a stress performance test in form of a thermal ramping, mussels were transferred from their aquaria into individual chambers (500 mL beakers, Duran, Germany) containing artificial seawater from the reservoir tanks at their respective treatment condition. Not all individuals could be measured simultaneously. Hence, thermal ramping trials were conducted on two consecutive days (days 13 and 14 after the start of exposure to the painted plates), using individuals from all treatment groups each day to minimize potential effects of exposure duration. In each chamber, gentle aeration was provided via a glass tube. In four chambers, loggers (Hobo Pendant Mx Temp) measuring temperature at a sampling rate of one reading per minute were attached to the tip of the glass tube which reached the bottom of the chamber. Chambers were placed in two water baths (Lauda Alpha RA24, Lauda-Brinkmann, Germany; n = 6–9 mussels per water bath). The next morning, 16 h after the transfer of mussels, the seawater was siphoned out and replaced with seawater from the respective reservoir to keep ammonia levels low (<0.25 mg/L, Test NH3/NH4, Tetra GmbH). One hour after the water exchange, the thermal ramping commenced by stepwise raising the temperature in the water baths by 1 °C every 15 min (4 °C/h) until 30 °C was reached (cf. Alter et al., 2025; Moyen et al., 2019). Heart rate, valve gape, and temperature were measured continuously at sampling rates as described above. Trials were conducted between 9 am and 4 pm in light conditions and without food supply in the same temperature-controlled room in which the coupon exposure took place. Salinity (range 33–34, WTW Multi 3620 IDS with TetraCon 925 electrode, Germany) and oxygen level (>95 % air saturation, WTW Multi 3620 IDS with FDO 925, Germany) were measured at the time the mussels were transferred to their individual chambers and at termination of the thermal ramping. After the trial was terminated, length, height, and width of the shell (Mitutoyo, Japan, ±0.01 mm), and wet weights of shell and tissue of individuals were determined (Model 1712 MP 8, Sartorius GmbH, Germany, precision 0.01 mg). Dry weights were determined after drying the tissue and shell in an oven at 100 °C for 48 h. The condition index (CI) was calculated by dividing the tissue dry weight (in mg) by the cube of the shell length (in cm).

2.3. Chemical analysis of leachates

Non-targeted chemical analysis was performed on seawater samples only and bivalve tissue was not analysed to confirm whether chemicals were taken up by the mussels. The seawater samples (approx. 200 mL) from the experiments were spiked with surrogate internal standards representing a range of volatilities (100 ng naphthalene-*d*8, 50 ng phenanthrene-*d*10, 50 ng chrysene-*d*12, 50 ng perylene-*d*12), pH adjusted to below 2 (using 15 % HCl), and extracted three times using dichloromethane (DCM, 30–15–15 mL). The combined organic extract was dried using anhydrous sodium sulphate and volume adjusted to approximately 500 µL using a gentle stream of nitrogen gas. A recovery standard (100 ng acenaphtene-*d*10 and 100 ng fluorene-*d*10) was added to all extracts prior to analysis.

Comprehensive two-dimensional gas chromatography–mass spectrometry (GC × GC–MS) analyses were performed using a 7890B GC coupled with a 7250 quadrupole time of flight mass spectrometer interfaced with a Zoex ZX2 cryogenic modulator. The first-dimension column was a Zebron ZB-1plus (30 m × 0.25 mm × 0.25 µm) and the second-dimension column was a BPX50 (1.0 m × 0.25 mm × 0.25 µm), interfaced by a 1 m × 0.25 mm deactivated fused silica modulation loop. The carrier gas was high purity helium at constant flow (1.1 mL/min). Samples (1 µL) were injected at 250 °C splitless. The oven temperature started at 60 °C (1 min hold) and was then ramped by 5 °C/min to 300 °C (10 min hold). The hot jet was offset starting at 10 °C (1 min hold) and was then ramped by 7 °C/min to 360 °C (10 min hold). The modulation time was 6 s with a 350 ms pulse length. The transfer line temperature was 300 °C, the ion source temperature was 200 °C, and the quadrupole temperature 150 °C. The electron ionization (EI) source was operated at 70 eV. Scan speed was 50 Hz and the recorded mass range was 50–650 *m/z*. A standard mixture (Table S1) was co-injected at least every ten samples.

MassHunter Unknowns Analysis software was applied to the raw data files for deconvolution and tentative identification of analytes as the best matches from the NIST17.L mass spectral library match with a similarity of >85 %. Additional parameters applied in the software is specified in Supplementary Material. Output files with all peaks, as well as with assigned tentative identities, were then exported to .csv format for further processing using R (R Development Core Team, 2021).

First dimension retention indexes (RIs) were calculated for all tentatively identified compounds (van Den Dool and Kratz, 1963). For GC × GC–MS, comparing first dimension RIs and second dimension absolute retention times predicted from physicochemical properties (automatically retrieved from PubChem using pubchempy) were used to filter out unlikely matches using partial least prediction (Sørensen et al., 2023a; Sørensen et al., 2023b), leaving only tentatively identified compounds with <200 deviation from predicted RI and <2 s absolute deviation of second dimension retention time. The resulting data set was investigated manually, and isomeric or similar mass spectral matches assigned at the same retention times (within 0.5 % deviation) were combined. Where total peak abundance was below the maximum of the laboratory blank samples (manual investigation), the data was removed from the data set during first prioritization. For compounds 'of interest' (detected in higher amounts in leachates than in controls), the peaks were re-introduced for preparation of time trend datasets. Where missing values were caused by a poorer match in some (less than half) of the leachates, these were also reintroduced if they were detected with a similarity >75 %. Compounds were included in the final data set if the average of all values in leachates met a set threshold criteria that was above 150 % of the average value observed in the control samples and they were detected with >85 % match in at least six of the leachate samples.

The peak response of the internal standards was used to monitor the stability and comparability of the extraction and analytical recoveries between samples and injections. Due to differences in the molecular and mass spectral properties of the internal standards and those of the tentatively identified chemicals, (semi-)quantification could not be performed.

2.4. Valve gape and heart rate analyses

The thickness of each mussel and the placement of the valve gape sensors on the margins of both valves influenced the strength of the electromagnetic field and, hence, the absolute distance between the two coils. The relationship between the strength of the field and the distance was calibrated to become linear by taking the square root of the reciprocal of each raw measurement. In this calibration, a value of 0 indicates a closed mussel and a value of 1 is the maximum distance measured between the coils (Ballesta-Artero et al., 2017). For the coupon

exposure, valve gape of each individual was averaged per day. For data from the performance stress test, valve gape was averaged across 5 min intervals. Broken stick regressions were then fitted to valve gape data in R (*respirometry*) to determine the breakpoint temperature (BPT), i.e. the temperature at which mussels closed their valves.

All data measured via the heart rate sensor were visually inspected (R, version 4.2.2) as the shape of the frequency curve may feature multiple peaks per heartbeat (Burnett et al., 2013). For the coupon exposure and stress test, the average heart rate was calculated for every 10 and 5 min interval, respectively.

Heart rate values across the different coupon exposures were used to construct frequency distribution histograms to estimate standard heart rates, similar to methods used for estimating standard metabolic rates (Fig. 1). The lowest and highest heart rate values of each individual were used to calculate 20 bins for which the histogram was determined. The peak of the distribution was considered as standard heart rate which was calculated for each experimental day (Steffensen et al., 1994). The lowest three bins of the histogram were used to calculate the time (fraction of day) during which blue mussels had an inactive heart rate. Heart rate data measured during the stress test were used to determine thermal performance curves (TPCs) which were fitted (*rTPC*, *nls.multstart*) in R using nonlinear least squares regression (Padfield et al., 2021). For this, five models, which included a performance maximum estimation in their formulation, were selected ("Gaussian_1987", "Joehnk_2008", "Oneill_1972", "Pawar_2018", "Weibull_1995"; Padfield et al., 2021). These five models were then weighted based on the smallest Akaike information criterion (AIC) and the temperature at which heart rate was maximal, as well as the maximum numerical value for heart rate was estimated. Q_{10} values were calculated from linear regressions fitted to individual heart rate at temperatures between 13 and 19 °C. Across this temperature range, heart rate was positively correlated with temperature in all individuals. For this, heart rates at two different temperatures were used, as described in Eq. 1:

$$Q_{10} = \left(\frac{R_2}{R_1}\right)^{\frac{10}{T_2 - T_1}} \quad (1)$$

where R_2 and R_1 are heart rates at high and low temperature (T_2, T_1), respectively.

2.5. Statistical analysis

To assess the drivers of valve gape and heart rate, i.e. presence of cardiac activity as well as standard heart rate during cardiac activity (bpm, log transformed), of *M. edulis* across the coupon exposure, hierarchical generalized additive models (HGAM) were ran using the *mgcv* package in RStudio (Pedersen et al., 2019; Wood, 2017). In each global model, experimental day was included using a smoother in an interaction with experimental treatment. Food was included as a fixed effect with two levels (whether mussels were fed on that day or not) and, in the standard heart rate model, tissue dry weight was included as a covariate. Individual mussels, nested in holding tanks, were accounted for as random intercepts. In alternative models, the possible effect of food was removed and the additive and interactive effects of treatment were removed. In the null model, only experimental day and nested individuals in tanks were included (Table S2). For the valve gape model, the average daily valve gape of each individual was used as response variable with a beta distribution and a logit link function. For the standard heart rate, a Gaussian distribution and identity link were used. For the time period of cardiac activity, it was registered every 10 min whether the heart rate was active or not (N = 144 measurements per day), and modelled using a binomial distribution and a logit link function. We assessed the overall frequency of active heart rate presence throughout the experimental period using a generalized linear mixed model (glmmTMB R package, Brooks et al., 2017). Treatment was included as fixed effect and tank as random intercept. A beta distribution and a logit link were used. We compared this model with one only including the random intercept through a likelihood ratio test. To explore the valve gape of *M. edulis* during the thermal stress test, HGAMs were fitted using a beta regression with a logit link. We tested whether temperature had a linear or non-linear effect on valve gape. In the non-linear alternative, we used a penalized spline (bs = "ps") with four or less knots to avoid overfitting. Models also included combinations of treatment and its interaction with temperature, and a random intercept for individuals. Inspection of the residuals indicated a poor fit of the full model and that individual mussels differed in their response to thermal stress. Hence, models that allowed individual-specific temperature effects were also assessed (Table S2).

To test for the effect of treatment on heart rate of *M. edulis* during the thermal stress test, we also fitted HGAMs. Owing to the strong influence of valve closure on heart rates (Fig. 1), heart rate data (bpm, log transformed) was compared between treatments only at temperatures below the BPT of valve gapes. Temperature and treatment were included in the models as described for valve gape. Individual mussels were accounted for as random intercepts and tissue dry weight was included as covariate (Table S2).

For all HGAM models, validation was done by visual inspection of quantile-quantile plots of deviance residuals, plots of deviance residuals against the predictors, and plots of observed versus fitted values. After validation, the best fitting model was identified based on the smallest AIC and, in case of insignificant differences between model fits (delta AIC < 2), the model with fewer predictor variables was chosen as the best fitting model (Table S2). Pairwise comparisons among treatments

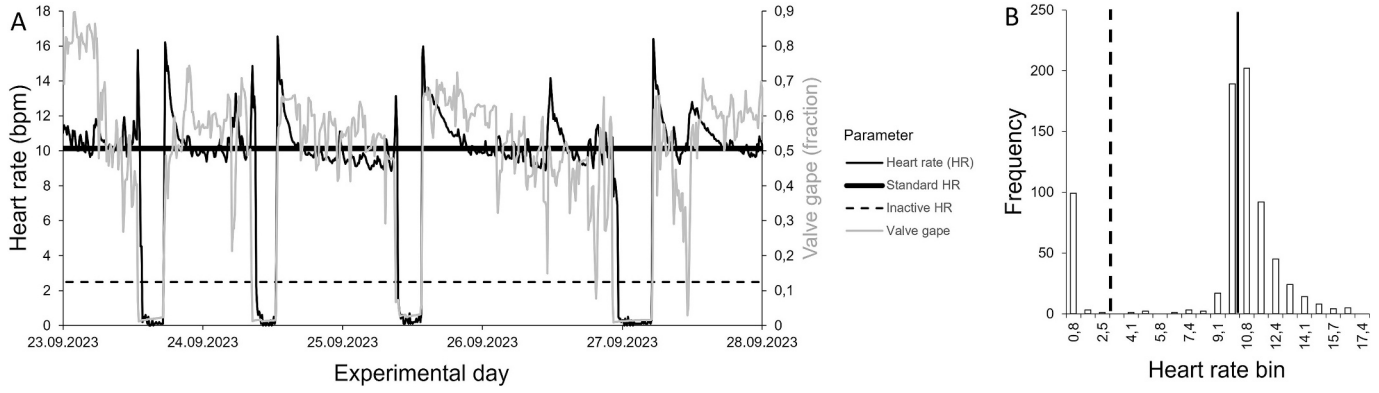

Fig. 1. (A) Example data of heart rate (bpm, black line) and valve gape (fraction, grey line) during coupon exposure. The thick black horizontal line indicates the standard heart rate and values below the dashed horizontal line were classified as inactive heart rates. Heart rate data were used to construct frequency histograms (B) from which standard (vertical solid line) and inactive heart rate (dashed vertical line) were estimated based on the peak and the three lowest bins of the distribution, respectively.

were conducted using *emmeans* package. *p*-Value adjustment was done with the Bonferroni method with a significance probability of <0.05.

To test if mussels used in different treatments had a different CI, a nested analysis of variances (ANOVA) was performed. Pearson correlation test was performed for data on BPT of valve gape and thermal optimum of heart rates. The correlation coefficients were then compared between treatment groups by applying the Fisher's *Z*-transformation. Other parameters calculated from data acquired during the stress test, i.e. thermal optimum for heart rate, maximum heart rate, Q_{10} values, and BPT of valve gape were used in one-way ANOVAs to test for differences among treatments. For ANOVA tests, normality was assessed using the Shapiro-Wilkinson test and homogeneity of variances was assessed using Levene's test.

All statistical analyses were conducted using RStudio (R Core Team, version 4.2.2). Data were graphically displayed with the *ggplot2* package (Wickham, 2016). All data in the text are stated as mean ± SE values.

3. Results

3.1. Chemical leachates

A total of 233 tentatively identified compounds (confidence in identification equivalent to level 3 of the Schymanski classification, Schymanski et al., 2014; adapted to GC–MS methodology, Koelmel et al., 2022) were detected in at least one of the leachate extracts, but 162 of these were also detected in control samples. For nine tentatively assigned compounds, the average of all values in the leachates met the set threshold criteria i.e. 150 % of the average value observed in the control samples and they were detected with >85 % match in at least six samples (Table 1). Additional diagnostic evidence (two-dimensional retention position) supports the identification, bringing it to level 2 confidence for those compounds where only one candidate structure was proposed. For the nine compounds, most displayed a maximum in relative abundance in leachates after 6 or 8 days, followed by a slight decline until the end of exposure (14 days) (Fig. S1).

3.2. Coupon exposure

Mussels used in the control, indirect, and direct exposure treatment had a similar CI of 62.2 ± 5.5, 56.9 ± 2.5, and 57.8 ± 3.8, respectively ($F_{(2,18)} = 0.479$, $p = 0.627$, Table S3). The best fitting model for valve gape (fraction) of *M. edulis* during the coupon exposure was the null model, including experimental day as smoother (HGAM; day: edf = 8.30, $\chi^2 = 184$, $p < 0.001$) and individual mussels as random effect (HGAM, edf = 22.3, $\chi^2 = 286.3$, $p < 0.001$, Table 2, Fig. 2, Tables S2 and S4). The deviance explained by the model was 73.1 % (Table 2).

The best fitting model for data on the time at which *M. edulis* had an active heart rate during the coupon exposure showed that the interaction between day and treatment, as well as individual variation (HGAM, edf = 24.339, $\chi^2 = 1478.1$, $p < 0.001$) played significant roles in explaining the response (Table 2, Fig. 3a, Tables S2 and S4). The interaction term had a significant non-linear relationship for the control treatment (HGAM, edf = 8.574, $\chi^2 = 1044.1$, $p < 0.001$), direct treatment (HGAM, edf = 8.707, $\chi^2 = 888.9$, $p < 0.001$), and indirect treatment (HGAM, edf = 8.723, $\chi^2 = 1009.6$, $p < 0.001$). Compared to the control treatment, the cardiac activity of mussels in the indirect treatment was arrested by 9 and 13 % more on days 3 and 10, respectively (HGAM, post-hoc, day 3: odds ratio = 3.077, SE = 0.571, $p \leq 0.001$; day 10: odds ratio = 1.741, SE = 0.293, $p = 0.035$), and by 8 and 12 % less on days 7 and 9, respectively (HGAM, post-hoc, day 7: odds ratio = 0.131, SE = 0.034, $p \leq 0.001$; day 9: odds ratio = 0.495, SE = 0.086, $p = 0.002$; Fig. 3a, Table S4). The cardiac arrest of mussels in the direct treatment occurred 12, 18 and 5 % more frequently than in control mussels on days 4, 10 and 11, respectively (HGAM, post-hoc, day 4: odds ratio = 2.536, SE = 0.483, $p \leq 0.001$; day 10: odds ratio = 2.137, SE = 0.384, $p = 0.001$; day 11: odds ratio = 2.301, SE = 0.424, $p < 0.001$), and 9 and 16 % less frequently on days 7 and 9, respectively (HGAM, post-hoc, day 7: odds ratio = 0.022, SE = 0.013, $p \leq 0.001$; day 9: odds ratio = 0.485, SE = 0.091, $p = 0.005$; Fig. 3a, Table S4). The deviance explained by the model was 68.1 % (Table 2). We did not find significant differences in

Table 2
Best generalized additive models of data of *Mytilus edulis* on **A** valve gape, **B** time of active heart rate, and **C** standard heart rate during metabolically active times across coupon exposure days, as well as on **D** valve gape and **E** standard heart rate during the thermal ramping. s() indicates that the variable is used as a smoother in the model. bs = "re" indicates that the smoothers are considered random effects.

Model specification	R^2	Deviance explained (%)
A valve gape ~ s(day) + s(tank, individual, bs = "re")	0.674	73.1
B time of active heart rate ~ s(day, by = treatment) + s(tank, individual, bs = "re")	0.633	68.1
C log(heart rate) ~ s(day) + s(tank, individual, bs = "re") + DW	0.808	83.0
D valve gape ~ s(temperature, by = individual, bs = "ps") + treatment	0.880	91.2
E log(heart rate) ~ s(temperature, by = treatment) + s(individual, bs = "re") + DW	0.875	88.2

Table 1
List of compounds detected with confidence and probable peak identity assigned in leachates. For some compounds, several plausible isomers are suggested, of which all are listed. Asterisks indicate properties that were sourced from the PubChem database. IUPAC = International Union of Pure and Applied Chemistry, CAS = Chemical Abstract Service registry number, CL = confidence level, MW = molecular weight, XlogP = predicted (PubChem) octanol/water partition coefficient logarithm form (proxy for the compound's hydrophobicity for neutral compounds), Rt = retention time, 1D = 1 dimensional chromatography, 2D = 2 dimensional chromatography, RI = retention index, Dev. = deviation, Det. Freq. = detection frequency.

IUPAC name	CAS	CL	MW (g/mol)*	XlogP*	Rt 1D (min)	Rt 2D (s)	RI	Dev. 1D Rt	Dev. 2D Rt	Det. Freq. (%)
2,3-Dihydroinden-1-one	83-33-0	2	132.2	1.7	13.82	3.42	1233	68	−1.0	100
1-(4-Methylphenyl)ethanol	536-50-5	2	136.2	1.8	11.06	1.94	1129	−119	−0.2	100
2-(4-Methylphenyl)propan-2-ol	1197-01-9	2	150.2	2	11.76	1.80	1156	165	−0.1	100
5,5-Dimethyl-4-(3-oxobutyl)oxolan-2-one	4436-81-1	2	184.2	0.7	20.22	3.82	1482	−113	−0.9	82
1-Bromo-2,4-dimethylbenzene	583-70-0	3	185.1	3.3	10.87	1.57	1122	159	−0.2	82
2-Bromo-1,3-dimethylbenzene	576-22-7			3.7						
1-Bromo-2,3-dimethylbenzene	576-23-8									
1,2-Dihydroacenaphthylene	83-32-9	2	154.2	3.9	16.81	2.47	1346	180	−0.6	64
1-(4-Methylphenyl)ethanone	122-00-9	2	134.2	2.1	11.45	2.29	1144	85	−0.3	55
1-Bromo-2,4,5-trimethylbenzene	5469-19-2576-83-0	3	199.1	3.7	15.41	1.92	1293	97	−0.1	64
2-Bromo-1,3,5-trimethylbenzene										
2,4-Dibromophenol	615-58-7	3	251.9	3.2	16.51	3.01	1335	31	−0.9	73
2,6-Dibromophenol	608-33-3			3.4						

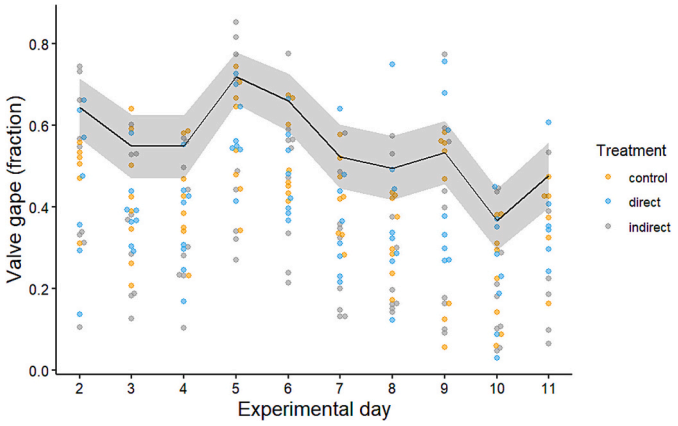

Fig. 2. Daily average valve gape (fraction) of *Mytilus edulis* across coupon exposure days. Jittered data are raw data of individual mussels that were exposed to seawater with chemical leachates from coatings used in offshore wind farms with (direct treatment, blue) and without (indirect treatment, grey) direct contact to coated plates and uncontaminated seawater (control, orange) (n = 8–9). The black line represents the population-level values with 95 % confidence interval (shaded area) predicted by the best model. (For interpretation of the references to colour in this figure legend, the reader is referred to the web version of this article.)

the overall frequency of active heart rate (likelihood ratio test: Chi sq = 4.44, $p = 0.11$, Fig. S2).

The best fitting model for data on standard heart rates of *M. edulis* during cardiac activity during the coupon exposure showed that a non-linear relationship with experimental day (HGAM, edf = 4.656, F = 7.071, $p < 0.001$), as well as a random intercept of individual mussels within aquaria (HGAM, edf = 2.326, F = 34.802, $p < 0.001$), affected the response (Table 2, Fig. 3b, Tables S2 and S4). The deviance explained by the model was 83.0 % (Table 2). Across coupon exposure days and treatments, the average standard heart rate of mussels varied between a maximum of 11.3 ± 0.4 bpm on day 2 and a minimum of 9.9 ± 0.3 bpm on day 4 (Fig. 3b).

3.3. Stress performance test

Valve openness of only the control and indirect exposure treatment could be analysed with sufficient replicate numbers (n = 6) due to equipment failure during the stress performance test.

The best fitting thermal performance curve model for valve gape, which included an interaction term for temperature with treatment and random intercepts for individual mussels, explained 91.2 % of the deviance (Table 2, Fig. 4a, Tables S2 and S4). Despite this, post-hoc comparisons assessing the difference in valve gape between control and exposed mussels were not significant for any temperature (Table S4).

The average BPT of valve gape was 19.2 ± 0.6 °C and was similar between treatments (ANOVA, $F_{(1,10)} = 0$, $p = 0.984$, Fig. 4b, Table S3). The thermal optimum and the maximum heart rate for mussels in the control (22.0 ± 0.8 °C, 21.1 ± 2.0 bpm), indirect (20.5 ± 0.9 °C, 20.4 ± 2.2 bpm) and direct (21.3 ± 1.0 °C, 23.5 ± 1.0 bpm) exposures were similar among treatments (ANOVA, thermal optimum: $F_{(2,21)} = 0.851$, $p = 0.441$, maximum heart rate: $F_{(2,21)} = 0.452$, $p = 0.642$, Table S3). Q_{10} values were similar among treatments (ANOVA, $F_{(2,21)} = 0.123$, $p = 0.885$) and ranged from 1.72 ± 0.1 to 1.78 ± 0.1 in the indirect and control treatments, respectively (Table S3). The BPT of valve gape was significantly correlated with the thermal optimum of heart rate of *M. edulis* for both the control (Pearson correlation coefficient (r) = 0.892) and indirect ($r = 0.912$) treatment with similar correlations between the two treatment groups (z-score = −0.133, $p = 0.894$, Fig. 4B).

The best fitting model for heart rates during the thermal stress test explained 88.2 % of the deviance (Table 2). It included a significant interaction term between temperature and treatment (HGAM, control: edf = 2.108, F = 207.6, $p < 0.001$, direct: edf = 1.000, F = 347.62, $p < 0.001$, indirect: edf = 1.061, F = 240.93, $p < 0.001$, Table S4) and significant individual variability between mussels (HGAM, edf = 20.784, F = 96.39, $p < 0.001$, Table S4). At each 1 °C temperature step, however, heart rates of mussels in the control treatment differed by a maximum of 0.6 and 1.3 bpm compared to those in the direct and indirect treatment, respectively (Fig. 4c, Table S4).

4. Discussion

Despite some differences in cardiac arrest patterns, exposure to chemical leachates from OWF coatings did not lead to significant changes in the parameters of mussel behaviour and physiology measured in this study during constant environmental conditions. The chemical exposure also did not lead to reductions in fitness endpoints, such as the temperature at which heart rate was maximal and the valves closed. The coated surface (58 cm^2) to volume of seawater (20 L) ratio used in the present study is roughly equivalent to a monopile spacing of

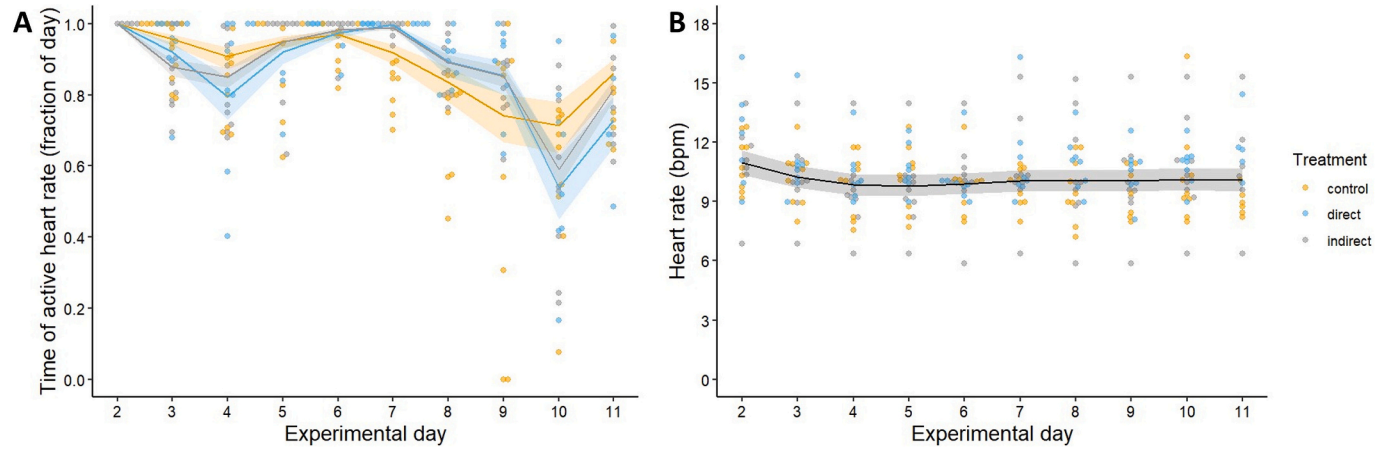

Fig. 3. (A) Time of active heart rate (fraction of day) and (B) standard heart rate (bpm) during metabolic active times of *Mytilus edulis*. Jittered dots are raw data of individual mussels that were exposed to seawater with chemical leachates from coatings used in offshore wind farms with (direct treatment, blue) and without (indirect treatment, grey) direct contact to coated plates and uncontaminated seawater (control, orange) (n = 8–9). Lines represent model predictions with a 95 % confidence interval (shaded area) on the treatment-level (A) and on the population-level (B). (For interpretation of the references to colour in this figure legend, the reader is referred to the web version of this article.)

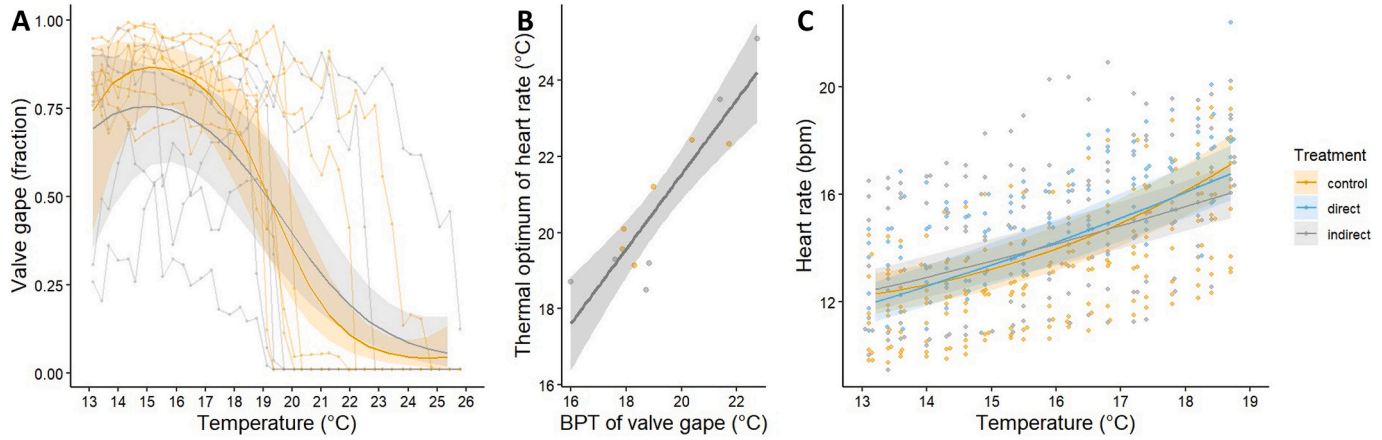

Fig. 4. (A) Valve gape (fraction) across temperatures (°C), (B) correlation between breakpoint temperature (BPT) of valve gape (°C) and thermal optimum of heart rate (°C), and (C) heart rate (bpm) at temperatures (°C) below the BPT of valve gape of *Mytilus edulis*. Mussels were exposed to seawater with chemical leachates from coatings used in offshore wind farms with (direct treatment, blue circles) and without (indirect treatment, grey circles) direct contact to coated plates and uncontaminated seawater (control, orange circles). Model predictions (lines) with 95 % confidence intervals (shaded area) for the effect of treatment are shown in A and C (colours). A regression line with 95 % confidence interval is shown for all treatments combined in B. Jittered dots are raw data points. n = 6 (A, B) and 7–9 (C). Insufficient n were available for valve gape data for the direct treatment (A, B). (For interpretation of the references to colour in this figure legend, the reader is referred to the web version of this article.)

8 m (assuming a 6 m diameter, 25 m water depth and square monopile spacing). Hence, the ratio used here led to potentially much higher leachate concentrations than any environmentally relevant conditions. Taken together, long-term impacts on mussel growth due to chemical leachates from OWF coatings under realistic exposure conditions are unlikely. Field studies are recommended to determine possible bioaccumulation of chemicals in the tissues of blue mussels and other species colonizing OWF structures. Further, future research on leachates from additional OWF components, such as sacrificial anodes, is needed to better understand the wider ecological risks and support sustainable OWF development.

Overall, few chemical compounds in the coating leachates were reliably detected in relative abundances above that of comparable control samples. In laboratory scale toxicity testing, high numbers of chemicals in control samples are common due to the ubiquitousness of chemicals in laboratory settings, in infrastructure, materials, equipment, air, and the seawater used for the studies. Within a certainty threshold, we discuss nine chemicals that are plausibly assigned to the coatings and have a probable identity assigned (Table 1). However, directly linking the proposed chemicals with uses in paints/coatings was not possible in all cases. This can be due to mis-assigned isomeric structures or a lack of openly available coating composition information. It is also plausible that compounds detected were present on the coated plates as contamination and not from the coating itself. 1-(4-methylphenyl)ethanol (CAS 536–50-5, also known as 1-(*p*-tolyl)ethanol) was the only compound detected in all leachate samples (replicates and timepoints) but in none of the controls. It presents in the class of branched alkyl phenols, a known constituent in paint coatings (PubChem database). Acenaphthene is a polycyclic aromatic hydrocarbon (PAH) with many uses, including in synthesis, dye, and paint production while dibromophenols are used as building blocks for flame retardant polymers (PubChem database, Kim and Oh, 2020).

Most of the detected chemical compounds leaching from the polymer-based coatings reached a relative abundance maximum after 6–8 days (Fig. S1), which is in line with previous observations for organic leachate kinetics from microplastic and rubber materials into seawater (Halsband et al., 2020; Sørensen et al., 2024). Of the nine identified chemicals, five of them have low xlogp values (<2.5) meaning they are likely to be too mobile for bioaccumulation to occur. The known toxicity data for the nine compounds to marine organisms varies, with halogenated aromatics (e.g., bromobenzenes, dibromophenols) and polycyclic aromatic hydrocarbons (PAHs, such as acenaphthene) posing the greatest risks due to their persistence, bioaccumulation, and toxicity to algae, invertebrates, and fish. Depending on their concentration, these compounds can cause acute and chronic effects, including growth inhibition, reproductive harm, and ecological damage (Honda and Suzuki, 2020; Michałowicz et al., 2022; Silva et al., 2024). Acenaphthene is recognized as 'substance of possible concern' under the OSPAR convention. It is also monitored as part of PAH groups by HELCOM. However, no Environmental Quality Standards for acenaphthene, bromobenzene, nor dibromophenol in marine waters are currently established under the EU Water Framework Directive, OSPAR, and HELCOM (OSPAR, 2023; HELCOM, 2018; European Council, 2013). Alcohols, ketones, and lactones are generally less toxic, with lower bioaccumulation potential and greater biodegradability, though they may still cause irritation or acute toxicity at high concentrations (Zicarelli et al., 2024).

The strategy for chemical analysis employed herein intentionally overlooks certain compound groups, particularly metals/inorganics and organics that are not extractable or amenable to GC-based techniques. This is a shortcoming of any screening methodology, and highlights the need for multiple techniques to be employed that fully cover the chemical space of compounds potentially leaching from OWF coatings (Hollender et al., 2023). Furthermore, the presence of contaminants in blank and control samples, combined with the strict removal of those features from reporting, means that some chemicals present at low levels may have been overlooked. It is therefore important to highlight that the presence of contaminants in the blank and control samples, and the approach implemented to address this may have influenced the resulting compound prioritization and toxicological data interpretation. Furthermore, it should be noted that only one coating formulation was tested in the current study and that further assessment of different coatings used within the OWF sector would provide a more comprehensive assessment of the potential chemical emissions and their impact on the marine environment. In the short-term, however, no adverse effects on heart rate and valve gape were detected and whether mussels accumulate any of the compounds leaching from coatings used in OWFs remains to be determined.

The heart rates of mussels were more constant than their valve gaping behaviour during the coupon exposure at constant temperatures. However, long periods of valve closure, i.e. a minimum of 0.5 h, were accompanied with cardiac arrest. Before long-term valve closures and

after their reopening, heart rate typically increased for short periods above the standard heart rate (cf. Trueman and Lowe, 1971). Thereby the overshoot when the valves reopen is due to an oxygen debt that builds up during closure (Trueman and Lowe, 1971 and references therein). Active heart rates were associated with valve gaping, but the degree of gaping or short-term closure did not influence heart rates, which is in agreement with previous reports (Trueman and Lowe, 1971; Curtis et al., 2000).

Although mussels maintained an active heart rate for most of the time, the duration of cardiac arrest episodes increased and the average valve gape decreased as the experimental period progressed. A gradual acclimation to the experimental tanks combined with low food supply may have resulted in the observed pattern (Riisgård et al., 2006). Bivalve valve gaping activity is strongly correlated with phytoplankton concentrations (Tang and Riisgård, 2016; Ballesta-Artero et al., 2017). By gradually closing their valve during low phytoplankton availability, *M. edulis* reduces both its filtration rate and respiration rate to conserve energy (Tang and Riisgård, 2016). Also the comparatively low numerical heart rate value (approx. 10 bpm at 13 °C) may indicate suboptimal nutrition. Widdows (1973) showed that *M. edulis* reduced its heart rate from 23 to 15 bpm during a one-month starvation period at 15 °C (Southern North Sea, Widdows, 1973). Other studies have reported *M. edulis* heart rates of 18 bpm at 15 °C (English Channel, Curtis et al., 2000) and 16 bpm (Southern North Sea, Alter et al., 2025; White Sea, Bakhmet et al., 2021) or 12 bpm at 10 °C (White Sea, Bakhmet et al., 2005).

Among groups, heart rate during active periods and valve gape were similar, yet cardiac arrest frequencies fluctuated non-monotonically across exposure days, with significant day-by-treatment interactions. Mussels in both, direct and indirect, exposure groups showed more pronounced shifts in cardiac arrest than controls, with steeper declines on days 4 and 10 and a sharper rebound on day 7. However, cumulative cardiac arrest time over the entire exposure duration was similar between treatments and controls, leading to a net equilibrium in activity (Fig. S2). Whether this temporal instability imposes longer-term physiological costs, such as reductions in health or growth, or is fully compensated over time, would benefit from longer-term monitoring or comparative studies. A recent study on the metal body burden of mussels suggests that exposure to leachates from OWF currently have no negative effects on health, as individuals originating from OWFs had similar condition indices compared to those from outside the OWF (Zonderman et al., 2025).

We used a non-targeted screening approach to identify as many leached compounds as possible, rather than to determine the concentration of specific compounds, so no direct comparison with environmental concentrations or potential toxicity estimates could be made. However, the coated surface to volume of seawater ratio used in our study likely resulted in much higher leachate concentrations than would be found under environmentally relevant conditions, even in a future ocean with abundant OWFs. The purpose of using an unrealistically high volume to surface ratio was to screen for potential toxicity from a novel, unknown, and understudied mixture of pollutants. This approach was intended as a first step to determine whether chemical leachates from paints warrant more detailed testing under environmentally realistic conditions. Therefore, our results should not be misinterpreted as directly indicative of real-world ecological risk without appropriate context. They are not suitable for setting environmental standards unless supported by studies using more representative leachate concentrations. It is also important to mention, that our study focused solely on organic paint leachates as part of the anti-corrosion protection system and did not include inorganic leachates, e.g. those derived from sacrificial anodes, which have been reported to cause toxic effects on marine organisms at concentrations often higher than those measured in the field (Kirchgeorg et al., 2018, Zonderman et al., 2025 and references herein). To comprehensively determine the impact of chemical leachates from OWFs, assessing the impact of organic leachates combined with galvanic and impressed current anodes is a logical next step.

When mussels were exposed to an additional driver, namely thermal stress, models that included an interaction term with treatment provided the best explanation for their heart rate and valve gape responses, albeit with insignificant post-hoc comparisons at all temperatures. For heart rates, differences were observed among treatments at different temperatures. Yet, the daily effect sizes were small, remaining below 1.3 bpm, suggesting that these differences are likely not biologically meaningful. Individual variability, by contrast, influenced all measured responses, also during constant temperature conditions. High inter-individual variability in mussels has been reported previously for heart rates, valve gaping, oxygen consumption rates, filtration rates, and growth under both stable and acutely increasing temperatures (Fernández-Reiriz et al., 2016; Hansen et al., 2024; Cheng et al., 2025). When predicting species responses to multiple driver conditions, it is important to further investigate the breadth of individual responses to better understand population-level effects. Varying biological responses interact with local environmental conditions and play a key role in shaping adaptive capacity in the face of environmental change (Tanner and Dowd, 2019).

Temperatures of valve gape breakpoints and maximal heart rates of *M. edulis* were similar to previous reports (21 and 25 °C, respectively, Southern North Sea, Alter et al., 2025). In the current study, leachate exposure did not reduce these fitness endpoints. This contrasts with our hypothesis that the combination of warming and leachate exposure would lower the upper thermal tolerance by causing an earlier onset of aerobic energy deficiency due to elevated energy demands for basal metabolism in chemically exposed mussels (e.g. Sokolova and Lannig, 2008; Bagwe et al., 2015; Op de Beeck et al., 2017). A reduced thermal tolerance due to chemical exposure has been reported previously for both aquatic invertebrates and vertebrates (reviewed in Sokolova and Lannig, 2008 and Monteiro et al., 2021). Although our results indicate no such effects, we cannot rule out the possibility that leachates subtly influence energy allocation of mussels. For example, a study on freshwater mussels showed that high chemical concentrations resulted in an energetic trade-off between detoxification at the cellular level and burrowing activity, even though metabolic rates, measured as oxygen consumption and heart rate, remained unchanged (Goodchild et al., 2016). Exploring metabolic shifts through cellular-level measurements or long-term growth studies could help determine whether exposure to leachates from the coatings used in OWFs affects mussel energy metabolism in ways not detectable through short-term fitness endpoints such as maximal heart rate or valve gape BPTs.

5. Conclusion

The current study showed that chemical leachates from coatings used in OWFs, under controlled laboratory conditions, did not induce measurable adverse effects on the heart rate and valve gape responses of *M. edulis*. Despite detecting several chemical compounds plausibly originating from the coatings, their presence (or the presence of other, non-detected or non-identified chemicals) did not correlate with significant deviations in mussel performance compared to controls. Even under additional thermal stress, responses remained within biologically insignificant margins, and individual variability played a larger role than treatment effects. It is important to note that while filtering criteria were applied, the limited number of tentatively identified compounds (levels 2–3) and the high background levels of contamination in controls constrain the generalizability of the findings, as does the inclusion of a single coat formulation in the study. As such, we cannot exclude the potential for subtle, long-term effects on energy allocation or bioaccumulation and suggest integrating cellular and population-level endpoints, including inorganic leachates from sacrificial anodes and other coating formulations in future studies. These efforts will be essential for evaluating the cumulative environmental footprint and assessing the sustainability of expanding OWFs in a changing ocean.

CRediT authorship contribution statement

Katharina Alter: Writing – review & editing, Writing – original draft, Visualization, Methodology, Funding acquisition, Formal analysis, Data curation, Conceptualization. **Moses Ndugwa:** Writing – review & editing, Investigation. **Paula de la Barra:** Visualization, Validation, Methodology, Formal analysis, Data curation. **Lieven Bervoets:** Writing – review & editing, Funding acquisition. **Gudrun De Boeck:** Writing – review & editing, Funding acquisition. **Andy M. Booth:** Writing – review & editing, Methodology, Funding acquisition, Formal analysis. **Lisbet Sørensen:** Writing – review & editing, Writing – original draft, Methodology, Investigation, Funding acquisition, Formal analysis, Data curation.

Declaration of competing interest

The authors declare that they have no known competing financial interests or personal relationships that could have appeared to influence the work reported in this paper.

Acknowledgements

This work was supported by the Interreg North Sea Programme 2021–2027 co-funded by the European Union Regional Development Fund under the project ANEMOI "Chemical emissions from offshore wind farms: assessing impacts, gaps and opportunities" with the grant agreement number 41-2-13-22.

Appendix A. Supplementary data

Supplementary data to this article can be found online at https://doi.org/10.1016/j.marpolbul.2025.118346.

Data availability

The data used and generated in this study have been deposited in the Zenodo database with DOI:10.5281/zenodo.15275276. The code used to perform this study are publicly available in the Zenodo database with DOI:10.5281/zenodo.15275276.

References

Abramic, A., Cordero-Penin, V., Haroun, R., 2022. Environmental impact assessment framework for offshore wind energy developments based on the marine Good Environmental Status. Environ. Impact Assess. Rev. 97, 106862. https://doi.org/10.1016/j.eiar.2022.106862.

Alava, J.J., Cheung, W.W., Ross, P.S., Sumaila, U.R., 2017. Climate change–contaminant interactions in marine food webs: toward a conceptual framework. Glob. Chang. Biol. 23 (10), 3984–4001. https://doi.org/10.1111/gcb.13667.

Alter, K., Constenla, M., Padrós, F., Sokolova, I.M., Born-Torrijos, A., 2025. Spawning is accompanied by increased thermal performance in blue mussels. J. Therm. Biol. 104018. https://doi.org/10.1016/j.jtherbio.2024.104018.

Bagwe, R., Beniash, E., Sokolova, I.M., 2015. Effects of cadmium exposure on critical temperatures of aerobic metabolism in eastern oysters *Crassostrea virginica* (Gmelin, 1791). Aquat. Toxicol. 167, 77–89. https://doi.org/10.1016/j.aquatox.2015.07.012.

Bakhmet, I., Fokina, N., Ruokolainen, T., 2021. Changes of heart rate and lipid composition in *Mytilus edulis* and *Modiolus modiolus* caused by crude oil pollution and low salinity effects. J. Xenobiot. 11 (2), 46–60. https://doi.org/10.3390/jox11020004.

Bakhmet, I.N., Berger, V.J., Khalaman, V.V., 2005. The effect of salinity change on the heart rate of *Mytilus edulis* specimens from different ecological zones. J. Exp. Mar. Biol. Ecol. 318 (2), 121–126. https://doi.org/10.1016/j.jembe.2004.11.023.

Ballesta-Artero, I., Witbaard, R., Carroll, M.L., van der Meer, J., 2017. Environmental factors regulating gaping activity of the bivalve *Arctica islandica* in Northern Norway. Mar. Biol. 164, 1–15. https://doi.org/10.1007/s00227-017-3144-7.

Bordalo, D., Cuccaro, A., Meucci, V., De Marchi, L., Soares, A.M., Pretti, C., Freitas, R., 2023. Will warmer summers increase the impact of UV filters on marine bivalves? Sci. Total Environ. 872, 162108. https://doi.org/10.1016/j.scitotenv.2023.162108.

Braby, C.E., Somero, G.N., 2006. Following the heart: temperature and salinity effects on heart rate in native and invasive species of blue mussels (genus *Mytilus*). J. Exp. Biol. 209 (13), 2554–2566. https://doi.org/10.1242/jeb.02259.

Brooks, M.E., Kristensen, K., van Benthem, K.J., Magnusson, A., Berg, C.W., Nielsen, A., Skaug, H.J., Maechler, M., Bolker, B.M., 2017. glmmTMB balances speed and flexibility among packages for zero-inflated generalized linear mixed modeling. R J. 9 (2), 378–400. https://doi.org/10.32614/RJ-2017-066.

Burnett, N.P., Seabra, R., de Pirro, M., Wethey, D.S., Woodin, S.A., Helmuth, B., Zippay, M.L., Sarà, G., Monaco, C., Lima, F.P., 2013. An improved noninvasive method for measuring heartbeat of intertidal animals. Limnol. Oceanogr. Methods 11 (2), 91–100. https://doi.org/10.4319/lom.2013.11.91.

Cheng, M.C., Ericson, J.A., Ragg, N.L., Dunphy, B.J., Zamora, L.N., 2025. Mussels, *Perna canaliculus*, as biosensors for climate change: concurrent monitoring of heart rate, oxygen consumption and gaping behaviour under heat stress. N. Z. J. Mar. Freshw. Res. 1–19. https://doi.org/10.1080/00288330.2025.2461757.

Curtis, T.M., Williamson, R., Depledge, M.H., 2000. Simultaneous, long-term monitoring of valve and cardiac activity in the blue mussel *Mytilus edulis* exposed to copper. Mar. Biol. 136, 837–846. https://doi.org/10.1007/s002270000297.

Degraer, S., Carey, D.A., Coolen, J.W.P., Hutchison, Z.L., Kerckhof, F., Rumes, B., Vanaverbeke, J., 2020. Offshore wind farm artificial reefs affect ecosystem structure and functioning: a synthesis. Oceanography 33 (4), 48–57. https://doi.org/10.5670/oceanog.2020.405.

van Den Dool, H., Kratz, P. Dec, 1963. A generalization of the retention index system including linear temperature programmed gas–liquid partition chromatography. J. Chromatogr. A 11, 463–471. https://doi.org/10.1016/S0021-9673(01)80947-X.

Durier, G., Nadalini, J.B., Saint-Louis, R., Genard, B., Comeau, L.A., Tremblay, R., 2021. Sensitivity to oil dispersants: effects on the valve movements of the blue mussel *Mytilus edulis* and the giant scallop *Placopecten magellanicus*, in sub-arctic conditions. Aquat. Toxicol. 234, 105797. https://doi.org/10.1016/j.aquatox.2021.105797.

Eom, S.H., Kim, S.S., Lee, J.B., 2020. Assessment of anti-corrosion performances of coating systems for corrosion prevention of offshore wind power steel structures. Coatings 10 (10), 970. https://doi.org/10.3390/coatings10100970.

European Council, 2013. Directive 2013/39/EU of the European Parliament and of the Council of 12 August 2013 amending Directives 2000/60/EC and 2008/105/EC as regards priority substances in the field of water policy. Off. J. Eur. Union 226, 1–17. Online. Assessed on 26 May 2025. https://eur-lex.europa.eu/legal-content/EN/ALL/?uri=CELEX%3A32013L0039.

Fernández-Reiriz, M.J., Irisarri, J., Labarta, U., 2016. Flexibility of physiological traits underlying inter-individual growth differences in intertidal and subtidal mussels *Mytilus galloprovincialis*. PLoS One 11 (2), e0148245. https://doi.org/10.1371/journal.pone.0148245.

Global Wind Energy Council, 2022. Global wind report 2022. Bonn, Germany. https://www.Annual-Wind-Report-2022_screen_final_April.pdf. gwec.net.

Goodchild, C.G., Frederich, M., Zeeman, S.I., 2016. Is altered behavior linked to cellular energy regulation in a freshwater mussel (*Elliptio complanata*) exposed to triclosan? Comp. Biochem. Physiol., Part C: Toxicol. Pharmacol. 179, 150–157. https://doi.org/10.1016/j.cbpc.2015.10.008.

Halldórsson, H.P., De Pirro, M., Romano, C., Svavarsson, J., Sarà, G., 2008. Immediate biomarker responses to benzo[a]pyrene in polluted and unpolluted populations of the blue mussel (*Mytilus edulis* L.) at high-latitudes. Environ. Int. 34 (4), 483–489. https://doi.org/10.1016/j.envint.2007.11.002.

Halsband, C., Sørensen, L., Booth, A.M., Herzke, D., 2020. Car tire crumb rubber: does leaching produce a toxic chemical cocktail in coastal marine systems? Front. Environ. Sci. 8, 557495. https://doi.org/10.3389/fenvs.2020.00125.

Hansen, G., Shumway, S.E., Mason, R.P., Baumann, Z., 2024. A comparative study of mercury bioaccumulation in bivalve molluscs from a shallow estuarine embayment. Arch. Environ. Contam. Toxicol. 86 (3), 262–273. https://doi.org/10.1007/s00244-024-01058-w.

Hartmann, J.T., Beggel, S., Auerswald, K., Stoeckle, B.C., Geist, J., 2016. Establishing mussel behavior as a biomarker in ecotoxicology. Aquat. Toxicol. 170, 279–288. https://doi.org/10.1016/j.aquatox.2015.06.014.

HELCOM, 2018. PAH and metabolites. HELCOM core indicator report. Online. Assessed on 26 May 2025. https://helcom.fi/wp-content/uploads/2019/08/Polyaromatic-hydrocarbons-PAHs-and-their-metabolites-HELCOM-core-indicator-2018.pdf.

Hengstmann, E., Pablo Zapata Corella, P., Alter, K., Belzunce-Segarra, M.J., Booth, A.M., Castro-Jiménez, J., Czerner, N., De Cauwer, K., Deviller, G., Gomiero, A., Goseberg, N., Hasenbein, S., Kirchgeorg, T., Mason, C., Pape, W., Parmentier, K., Plaß, A., Pröfrock, D., Sarhadi, A., Vanavermaete, D., van der Molen, J., Almeida Vinagre, P., Wood, D., Weinberg, I., Wind, C., Zonderman, A., Kenyon, J., de Witte, B., 2025. Chemical emissions from offshore wind farms: from identification to challenges in impact assessment and regulation. Mar. Pollut. Bull. 215, 117915. https://doi.org/10.1016/j.marpolbul.2025.117915.

Hollender, J., Schymanski, E.L., Ahrens, L., Alygizakis, N., Béen, F., Bijlsma, L., Brunner, A.M., Celma, A., Fildier, A., Fu, Q., Gago-Ferrero, P., Gil-Solsona, R., Haglund, P., Hansen, M., Kaserzon, S., Kruve, A., Lamoree, M., Margoum, C., Meijer, J., Merel, S., Rauert, C., Rostkowski, P., Samanipour, S., Schulze, B., Schulze, T., Singh, R.R., Slobodnik, J., Steininger-Mairinger, T., Thomaidis, N.S., Togola, A., Vorkamp, K., Vulliet, E., Zhu, L., Krauss, M., 2023. NORMAN guidance on suspect and non-target screening in environmental monitoring. Environ. Sci. Eur. 35 (1), 75. https://doi.org/10.1186/s12302-023-00779-4.

Honda, M., Suzuki, N., 2020. Toxicities of polycyclic aromatic hydrocarbons for aquatic animals. Int. J. Environ. Res. Public Health 17 (4), 1363. https://doi.org/10.3390/ijerph17041363.

Kasiotis, K.M., Emmanouil, C., Anastasiadou, P., Papadi-Psyllou, A., Papadopoulos, A., Okay, O., Machera, K., 2015. Organic pollution and its effects in the marine mussel *Mytilus galloprovincialis* in Eastern Mediterranean coasts. Chemosphere 119, S145–S152. https://doi.org/10.1016/j.chemosphere.2014.05.078.

Kholodkevich, S.V., Kuznetsova, T.V., Trusevich, V.V., Kurakin, A.S., Ivanov, A.V., 2009. Peculiarities of valve movement and of cardiac activity of the bivalve mollusc *Mytilus galloprovincialis* at various stress actions. J. Evol. Biochem. Physiol. 45 (4), 52–526. https://doi.org/10.1134/S0022093009040100.

Kim, U.J., Oh, J.E., 2020. Environmental occurrence and behaviour of BFR structural analogues and metabolites. Compr. Anal. Chem. 88, 253–301. https://doi.org/10.1016/bs.coac.2019.10.006.

Kirchgeorg, T., Weinberg, I., Hörnig, M., Baier, R., Schmid, M.J., Brockmeyer, B., 2018. Emissions from corrosion protection systems of offshore wind farms: evaluation of the potential impact on the marine environment. Mar. Pollut. Bull. 136, 257–268. https://doi.org/10.1016/j.marpolbul.2018.08.058.

Koelmel, J.P., Xie, H., Price, E.J., Lin, E.Z., Manz, K.E., Stelben, P., Paige, M.K., Papazian, S., Okeme, J., Jones, D.P., Barupal, D., Bowden, J.A., Rostkowski, P., Pennell, K.D., Nikiforov, V., Wang, T., Hu, X., Lai, Y., Miller, G.W., Walker, D.I., Martin, J.W., Godri Pollitt, K.J., 2022. An actionable annotation scoring framework for gas chromatography-high-resolution mass spectrometry. Exposome 2, osac007. https://doi.org/10.1093/exposome/osac007.

Maulvault, A.L., Camacho, C., Barbosa, V., Alves, R., Anacleto, P., Fogaça, F., Kwadijk, C., Kotterman, M., Cunha, C.S., Fernandes, J.O., Rasmussen, R.R., Sloth, J. J., Aznar-Alemany, O., Eljarrat, E., Barceló, D., Marques, A., 2018. Assessing the effects of seawater temperature and pH on the bioaccumulation of emerging chemical contaminants in marine bivalves. Environ. Res. 161, 236–247. https://doi.org/10.1016/j.envres.2017.11.017.

Michałowicz, J., Włuka, A., Bukowska, B., 2022. A review on environmental occurrence, toxic effects and transformation of man-made bromophenols. Sci. Total Environ. 811, 152289. https://doi.org/10.1016/j.scitotenv.2021.152289.

Monteiro, D.A., Kalinin, A.L., Rantin, F.T., McKenzie, D.J., 2021. Use of complex physiological traits as ecotoxicological biomarkers in tropical freshwater fishes. J. Exp. Zool. Pt. A Ecol. Integr. Physiol. 335 (9–10), 745–760. https://doi.org/10.1002/jez.2540.

Moyen, N.E., Somero, G.N., Denny, M.W., 2019. Impact of heating rate on cardiac thermal tolerance in the California mussel, *Mytilus californianus*. J. Exp. Biol. 222 (17), jeb203166. https://doi.org/10.1242/jeb.203166.

Nardi, A., Mincarelli, L.F., Benedetti, M., Fattorini, D., d'Errico, G., Regoli, F., 2017. Indirect effects of climate changes on cadmium bioavailability and biological effects in the Mediterranean mussel *Mytilus galloprovincialis*. Chemosphere 169, 493–502. https://doi.org/10.1016/j.chemosphere.2016.11.093.

Noyes, P.D., Lema, S.C., 2015. Forecasting the impacts of chemical pollution and climate change interactions on the health of wildlife. Curr. Zool. 61 (4), 669–689. https://doi.org/10.1093/czoolo/61.4.669.

Op de Beeck, L., Verheyen, J., Stoks, R., 2017. Integrating both interaction pathways between warming and pesticide exposure on upper thermal tolerance in high-and low-latitude populations of an aquatic insect. Environ. Pollut. 224, 714–721. https://doi.org/10.1016/j.envpol.2016.11.014.

OSPAR, 2023. OSPAR list of chemicals for priority action. OSPAR convention for the protection of the marine environment of the north-east Atlantic. Online. Assessed on 25 May 2025. https://www.ospar.org/work-areas/hasec/hazardous-substances/priority-action.

Padfield, D., O'Sullivan, H., Pawar, S., 2021. rTPC and nls. multstart: a new pipeline to fit thermal performance curves in R. Methods Ecol. Evol. 12 (6), 1138–1143. https://doi.org/10.1111/2041-210X.13585.

Pedersen, E.J., Miller, D.L., Simpson, G.L., Ross, N., 2019. Hierarchical generalized additive models in ecology: an introduction with mgcv. PeerJ 7, e6876. https://doi.org/10.7717/peerj.6876.

Price, S.J., Figueira, R.B., 2017. Corrosion protection systems and fatigue corrosion in offshore wind structures: current status and future perspectives. Coatings 7 (2), 25. https://doi.org/10.3390/coatings7020025.

Riisgård, H.U., Larsen, P.S., 2015. Physiologically regulated valve-closure makes mussels long-term starvation survivors: test of hypothesis. J. Molluscan Stud. 81 (2), 303–307. https://doi.org/10.1093/mollus/eyu087.

Riisgård, H.U., Lassen, J., Kittner, C., 2006. Valve-gape response times in mussels (*Mytilus edulis*)—effects of laboratory preceding-feeding conditions and in situ tidally induced variation in phytoplankton biomass. J. Shellfish Res. 25 (3), 901–911. https://doi.org/10.2983/0730-8000(2006)25[901:VRTIMM]2.0.CO;2.

Schymanski, E.L., Jeon, J., Gulde, R., Fenner, K., Ruff, M., Singer, H.P., Hollender, J., 2014. Identifying small molecules via high resolution mass spectrometry: communicating confidence. Environ. Sci. Tech. 48, 2097–2098. https://doi.org/10.1021/es5002105.

Silva, D.C.C., Marques, J.C., Gonçalves, A.M.M., 2024. Polycyclic aromatic hydrocarbons in commercial marine bivalves: abundance, main impacts of single and combined exposure and potential impacts for human health. Mar. Pollut. Bull. 209, 117295. https://doi.org/10.1016/j.marpolbul.2024.117295.

Sokolova, I.M., Lannig, G., 2008. Interactive effects of metal pollution and temperature on metabolism in aquatic ectotherms: implications of global climate change. Clim. Res. 37 (2–3), 181–201. https://doi.org/10.3354/cr00764.

Sørensen, L., Schaufelberger, S., Igartua, A., Størseth, T.R., Øverjordet, I.B., 2023a. Non-target and suspect screening reveal complex pattern of contamination in arctic marine zooplankton. Sci. Total Environ. 864, 161056. https://doi.org/10.1016/j.scitotenv.2022.161056.

Sørensen, L., Gomes, T., Igartua, A., Lyngstad, I.L., Almeida, A.C., Wagner, M., Booth, A. M., 2023b. Organic chemicals associated with rubber are more toxic to marine algae and bacteria than those of thermoplastics. J. Hazard. Mater. 458, 131810. https://doi.org/10.1016/j.jhazmat.2023.131810.

Sørensen, L., Zammite, C., Igartua, A., Christensen, M.M., Haraldsvik, M., Creese, M., Gomes, T., Booth, A.M., 2024. Towards realism in hazard assessment of plastic and rubber leachates—methodological considerations. J. Hazard. Mater. 480, 136383. https://doi.org/10.1016/j.jhazmat.2024.136383.

Steffensen, J.F., Bushnell, P.G., Schurmann, H., 1994. Oxygen consumption in four species of teleosts from Greenland: no evidence of metabolic cold adaptation. Polar Biol. 14, 49–54. https://doi.org/10.1007/BF00240272.

Tang, B., Riisgård, H.U., 2016. Physiological regulation of valve-opening degree enables mussels *Mytilus edulis* to overcome starvation periods by reducing the oxygen uptake. Open J. Mar. Sci. 6 (3), 341–352. https://doi.org/10.4236/ojms.2016.63029.

Tanner, R.L., Dowd, W.W., 2019. Inter-individual physiological variation in responses to environmental variation and environmental change: integrating across traits and time. Comp. Biochem. Physiol. A Mol. Integr. Physiol. 238, 110577. https://doi.org/10.1016/j.cbpa.2019.110577.

Tran, D., Andrade, H., Durier, G., Ciret, P., Leopold, P., Sow, M., Ballantine, C., Camus, L., Berge, J., Perrigault, M., 2020. Growth and behaviour of blue mussels, a re-emerging polar resident, follow a strong annual rhythm shaped by the extreme high Arctic light regime. R. Soc. Open Sci. 7 (10), 200889. https://doi.org/10.1098/rsos.200889.

Trueman, E.R., Lowe, G.A., 1971. The effect of temperature and littoral exposure on the heart rate of a bivalve mollusc, *Isognomum alatus*, in tropical conditions. Comp. Biochem. Physiol. A Physiol. 38 (3), 555–564.

Turja, R., Höher, N., Snoeijs, P., Baršienė, J., Butrimavičienė, L., Kuznetsova, T., Kholodkevich, S.V., Devier, M.H., Budzinski, H., Lehtonen, K.K., 2014. A multibiomarker approach to the assessment of pollution impacts in two Baltic Sea coastal areas in Sweden using caged mussels (*Mytilus trossulus*). Sci. Total Environ. 473, 398–409. https://doi.org/10.1016/j.scitotenv.2013.12.038.

Wickham, H., 2016. ggplot2: Elegant Graphics for Data Analysis. Springer-Verlag New York.

Widdows, J., 1973. The effects of temperature on the metabolism and activity of *Mytilus edulis*. Neth. J. Sea Res. 7, 387–398. https://doi.org/10.1016/0077-7579(73)90060-4.

Wood, S.N., 2017. Generalized Additive Models: An Introduction With R, 2nd ed. CRC. https://doi.org/10.1201/9781315370279.

Yu, M., Fan, C., Ge, F., Lu, Q., Wang, X., Cui, Z., 2021. Anticorrosion behavior of organic offshore coating systems in UV, salt spray and low temperature alternation simulated Arctic offshore environment. Mater. Today Commun. 28, 102545. https://doi.org/10.1016/j.mtcomm.2021.102545.

Zicarelli, G., Faggio, C., Balhova, J., Riesova, B., Hesova, R., Doubkova, V., Svobodova, Z., Lakdawala, P., 2024. Toxicity of water-soluble polymers polyethylene glycol and polyvinyl alcohol for fish and frog embryos. Sci. Total Environ. 933, 173154. https://doi.org/10.1016/j.scitotenv.2024.173154.

Zonderman, A., Wipperman, D., Ebeling, A., Klein, O., Erbslöh, H.B., Zimmermann, T., Hildebrandt, L., Hasenbein, S., Weinberg, I., Kirchgeorg, T., Pröfrock, D., 2025. Analyzing the metal body burden of turbine-colonizing mussels from North Sea offshore wind farms. Mar. Pollut. Bull. 218, 118216. https://doi.org/10.1016/j.marpolbul.2025.118216.